Chinese Journal of Chemical Engineering 29 (2021) 85–91

Contents lists available at ScienceDirect

Chinese Journal of Chemical Engineering

journal homepage: www.elsevier.com/locate/CJChE

Article

Spray coating of polysulfone/poly(ethylene glycol) block polymer on macroporous substrates followed by selective swelling for composite ultrafiltration membranes

Dongwei Ma [1], Zhaogen Wang [1], Tao Liu [2], Yunxia Hu [2], Yong Wang [1,*]

[1] State Key Laboratory of Materials-Oriented Chemical Engineering, College of Chemical Engineering, Nanjing Tech University, Nanjing 211816, China
[2] State Key Laboratory of Separation Membranes and Membrane Processes, School of Materials Science and Engineering, Tiangong University, Tianjin 300387, China

ARTICLE INFO

Article history:
Received 12 March 2020
Received in revised form 12 April 2020
Accepted 3 May 2020
Available online 21 May 2020

Keywords:
Spray coating
Polysulfone
Block copolymers
Selective swelling
Ultrafiltration membranes

ABSTRACT

Polysulfone (PSF) is extensively used for the production of ultrafiltration (UF) membranes thanks to its high strength, chemical stability, and good processibility. However, PSF is intrinsically hydrophobic, and hydrophilic modification is always required to PSF-based membranes if they are intended to be used in aqueous systems. Facile strategies to prepare hydrophilic PSF membranes are thus highly demanded. Herein we spray coat a PSF-based amphiphilic block polymer onto macroporous substrates followed by selective swelling to prepare flat-sheet PSF UF membranes. The polymer is a triblock polymer containing PSF as the majority middle block tethered with shorter block of polyethylene glycol (PEG) on both ends, that is, PEG-*b*-PSF-*b*-PEG. We use the technique of spray coating to homogeneously dispense diluted triblock polymer solutions on the top of macroporous supports, instantly resulting in uniform, defect-free polymer coating layers with the thickness down to ~1.2 μm. The bi-layered composite structures are then immerged in ethanol/acetone mixture to generate mesoscale pores in the coating layers following the mechanism of selective swelling-induced pore generation, thus producing composite membranes with the mesoporous triblock polymer coating as the selective layers. This facile strategy is free from additional hydrophilic modification and much smaller dosages of polymers are used compared to conventional casting methods. The pore sizes, porosities, hydrophilicity, and consequently the separation properties of the membranes can be flexibly tuned by changing the swelling duration and the composition of the swelling bath. This strategy combining spray coating and selective swelling is upscalable for the production of high-performance PSF UF membranes.

1. Introduction

Polymeric membranes have occupied most of the membrane markets in water purification and desalination, largely owing to their high processability, low cost, and the broad sources of polymers [1,2]. A variety of polymers, including cellulose acetate (CA), polyimides (PI), polyacrylonitrile (PAN), poly(vinylidene fluoride) (PVDF), polyamides (PA), polyethersulfone (PES) and polysulfone (PSF) *etc.*, have been utilized to fabricate reverse osmosis (RO), nanofiltration (NF), ultrafiltration (UF) and microfiltration (MF) membranes. The choice of polymers directly determines the final membrane performances. Specifically, as one polymeric material with good chemical resistance, mechanical stability, thermostability and relatively low cost [3], PSF is widely used for the fabrication of UF membranes. However, a common concern of PSF membranes lies in the hydrophobic nature of PSF, which can lead to fast membrane fouling and consequently shorten the lifetime of membranes in water purification [4]. There are many physical and chemical approaches to improve the hydrophilicity and anti-fouling ability of PSF membranes [5–7], among which incorporation of hydrophilic additives is one popular and simple strategy. Hydrophilic polymeric additives, such as polyethylene glycol (PEG) [8–10], polyvinylpyrrolidone (PVP) [11], propionic acid [12], and polyaniline (PANI) [13,14] were added in the membrane fabrication recipes to promote the fluxes as well as fouling resistance of PSF membranes. Due to its high hydration capacity, biocompatibility and easy accessibility with tunable molecular weights, PEG has been gaining particular interest and is widely used to modify PSF membranes. However, the poor miscibility and attachment between PEG and PSF membranes by physical mixing can cause leaching problem [15,16].

Using PSF based graft copolymers (PSF-*g*-PEG) or block copolymers (PSF-*b*-PEG) as additives can promote their adhesion with PSF membranes and reduce the possible leaching out of PEG components. Many researchers fabricated UF membranes by blending PSF-*g*-PEG or PSF-*b*-PEG in PSF casting recipes during nonsolvent induced phase separation (NIPS), a traditional membrane preparation method with simplicity and

* Corresponding author.
E-mail address: yongwang@njtech.edu.cn (Y. Wang).

https://doi.org/10.1016/j.cjche.2020.05.002
1004-9541/

controllability for industrial applications [17,18]. Thus-obtained blend membranes exhibited much higher permeance and better fouling resistance than PSF bare membranes. Using pure PSF-*b*-PEG polymers is an alternative way to prepare PSF based UF membranes [19,20]. The chemical bond between PSF and PEG phases can guarantee their strong affinity and completely avoid the leaching out of PEG components during use. Besides, owing to the additional water channel provided by the continuous PEG microdomains and the promoted PEG distribution on membrane surface, PSF-*b*-PEG membranes can show further enhanced permeability and fouling resistance. In our previous work, we have also prepared porous PSF-*b*-PEG membranes based on selective swelling induced pore generation in the pair of a PSF-selective solvent and a PEG-selective solvent [21,22]. The membranes possessed interconnected mesopores with enhanced hydrophilicity and anti-fouling property because of the presence of PEG chains along the pore wall. This swelling strategy is facile and controllable by adjusting the compositions of the solvent pair and the swelling temperature/durations. Moreover, compared to NIPS, much thinner PSF-*b*-PEG layers can be achieved by swelling. However, although several methods to prepare BCP membranes have been exploited [23,24], how to manufacture PSF-*b*-PEG membranes at large scale with an effective and easy-to-operate technology remains unaddressed.

Recently, we employed spray coating enabled film formation for preparation of BCP composite membranes and fabricated polystyrene-*block*-poly(2-vinylpyridine) (PS-*b*-P2VP) membranes by coupling spray coating with selective swelling [25]. The spray coating technique is frequently used to construct thin films on different substrates and possesses various advantages including low-cost production, high utilization of polymers and no limitation for substrate sizes or shapes [26–29]. It also shows great potential for mass volume manufacturing. Here in this study, we attempt to fabricate PSF/PEG block polymer (abbreviated as SFEG) membranes on macroporous supports by spray coating and selective swelling. Distinguished from PS-*b*-P2VP, SFEG has a higher mechanical strength and hydrophilicity, and their spray coating conditions are different. The thicknesses, structures and properties of the active layers under different coating/swelling conditions, which play a vital role in membrane separation [30,31], are studied. By taking the advantages of SFEG polymers, spray coating as well as selective swelling, a systematic fabrication process for UF membranes with tunable and superior performances is expected. Larger-area fabrication of SFEG membranes is discussed.

2. Experimental

2.1. Materials

The PSF-based triblock polymer, polyethylene glycol-*block*-polysulfone-*block*-polyethylene glycol (PEG-*b*-PSF-*b*-PEG, abbreviated as SFEG) was synthesized *via* aromatic nucleophilic substitution according to the reported protocol [32] and monomethylpoly(ethylene glycol) (mPEG, M_n: 6 kg·mol^{-1}) was used to synthesize SFEG. The number-average molecular weight (M_n) of SFEG was 23,000 with PDI = 1.52, and the weight ratio of PEG in the SFEG was 22 wt%. Analytically pure grade 1,2-dichloroethane (≥99.0%), acetone (≥99.5%) and ethanol (≥99.7%) were purchased from Shanghai Lingfeng Chemical Regent Co., Ltd. Bovine serum albumin (BSA, purity of 98%) with a molecular weight of 66,000 and phosphate buffer solutions (PBS) tablets were purchased from MP Biomedicals, LLC. PBS solutions with a pH of 7.4 were obtained by dissolving one phosphate tablet in 100 ml deionized water. Dilute aqueous solutions of monodispersed 15-nm gold colloid were purchased from British Biocell International Limited. Nylon microfiltration membranes with a nominal pore size of ~0.8 μm were purchased from Haining Shenghua Filtration Equipment Co., Ltd. and used as the supports to prepare composite membranes. Deionized water (conductivity: 8–20 μs·cm^{-1}) was used in all experiments. All regents were used without further purification.

2.2. Membrane preparation

During spray coating, a series of parameters can influence the film thickness and morphology, including polymer concentration, solution viscosity, air pressure, the distance between nozzle and heating plate [33], the temperature of heating plate [26,33], step width [25], environment humidity and so on. Some of these parameters also have mutual effects with each other. In this study, different factors were optimized and determined for the sake of fabricating thin and defect-free SFEG composite membranes. The spray apparatus (SEV-300EDN, Suzhou Second Automatic Equipment Co., Ltd) was positioned in a fume hood, and the humidity was controlled in the range of 30%–50% to prevent undesired macropores on membrane surface caused by environmental humidity. The spray distance between nozzle and heating plate was maintained at 62 mm and the temperature of heating plate was 25 °C. Firstly, SFEG was dissolved in 1,2-dichloroethane with a concentration of 3 wt% at room temperature with the assistance of ultrasonication. Nylon microfiltration membranes with a size of 5 cm × 5 cm were attached onto the horizontal heating plate of the spray setup. Afterwards, the SFEG solutions were poured into the reservoir of spray setup and then atomized and uniformly deposited onto the nylon microfiltration membranes. As shown in Fig. 1(a), the macroporous support was completely covered by SFEG *via* spray coating. Thus-produced composite membranes, composed of SFEG layers and nylon supports, were immersed in the ethanol/acetone paired solvents for desired durations and then taken out and dried at room temperature to cavitate pores through the SFEG layers. SFEG composite membranes with larger area (30 cm × 30 cm) were fabricated under the same conditions as described above.

2.3. Characterizations

A field-emission scanning electron microscope (FE-SEM, Hitachi S4800) was used to detect both the surface and cross-sectional morphologies of the composite membranes at an accelerating voltage of 5 kV. Energy Dispersive X-ray Analysis (EDX) was performed at an accelerating voltage of 20 kV and electric current of 10 mA. The membranes were quick-frozen by soaking in liquid nitrogen and ruptured to obtain the samples for cross-sectional observation. All samples were sputter-coated with gold for 20 s to avoid charging effects prior to SEM characterizations. The thicknesses of SFEG layers were determined by data statistics according to the cross-sectional SEM images. As the expansion of SFEG polymer chains was confined in the vertical direction while the horizonal movements were limited by substrates. Porosities of the SFEG layers can be roughly calculated by the Eq. (1):

$$P = 100\% \times t - t_0/t \quad (1)$$

where t_0 and t were the thicknesses of SFEG layers before and after swelling.

Data statistics of at least 100 pores by the surface SEM image of each sample were conducted to estimate the average pore size. An angle goniometer (DropMeter A-100, Maist) was employed to analyze the surface hydrophilicity of composite membranes. For each sample, at least 5 positions were measured and the average value of the dynamic water contact angle (DWCA) was reported.

2.4. Filtration tests

Membrane performances were evaluated by a cross-flow apparatus (SF-SA, Hangzhou Saifei Membrane Separation Technique Co., Ltd.). Prior to filtration tests, pre-compaction of the composite membranes was carried out at the pressure of 0.15 MPa to ensure a stable flux. Water flux tests were performed at the pressure of 0.1 MPa and the effective area of the membrane is 7.1 cm^2. BSA solutions with a

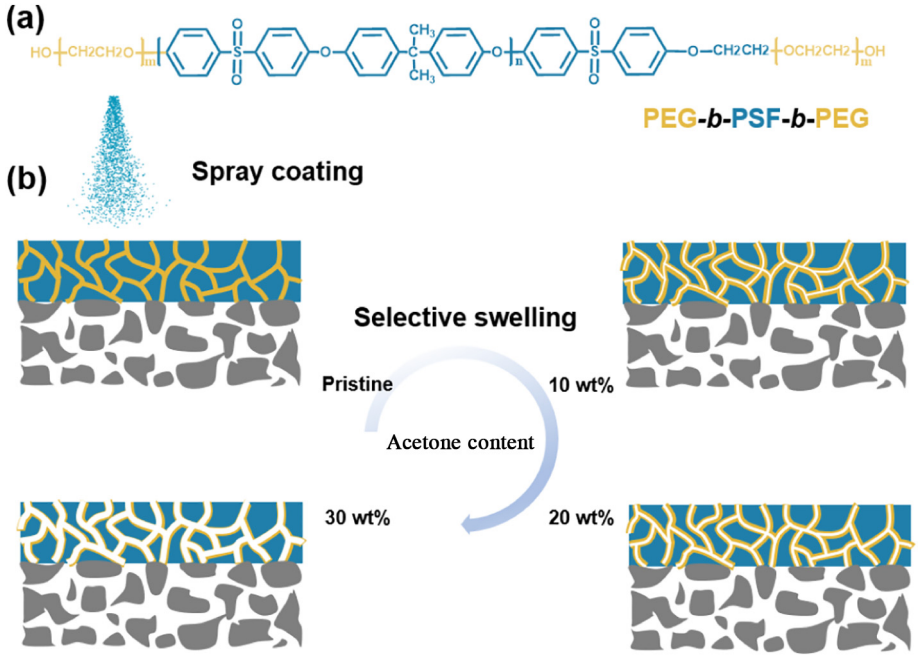

Fig. 1. (a) Molecular structure of the PEG-*b*-PSF-*b*-PEG triblock polymer. (b) Illustration for preparation of SFEG composite membranes by spray coating and selective swelling in different paired solvents

concentration of 0.5 $g \cdot L^{-1}$ and dilute aqueous solutions of monodispersed gold colloid nanoparticles were used to illuminate the exclusion ability of SFEG membranes. The BSA and gold colloid nanoparticles concentrations in feed solutions, filtrates and retentates were detected by a UV–vis absorption spectrometer (NanoDrop2000c, Thermo). The rejection rates of BSA or gold colloid were calculated according to the Eq. (2):

$$R = 100\% \times (1 - C_p/C_f) \quad (2)$$

where C_p and C_f are the concentrations of BSA/gold colloid nanoparticles in the filtrates and the feed aqueous solutions, respectively.

3. Results and Discussion

3.1. Preparation of SFEG composite membranes

The spray coating procedure was almost the same as our previous work [25]. After a series of preliminary investigations, the optimized conditions were determined as follows: SFEG solutions in 1,2-dichloroethane with a concentration of 3 wt% were extruded from the spray needle and deposited onto nylon supports. After coating and solvent evaporation, the initially macroporous nylon support (Fig. 2(a) and (c)) was fully covered by a thin, dense and defect-free layer (Fig. 2(b) and (d)) derived from the SFEG solutions. A small amount of SEFG solutions penetrated into the nylon support (Fig. 2(d)). By controlling the amounts of deposited SFEG solutions, the thickness of the final SFEG films can be decreased as thin as 1.2 μm on the premise of maintaining the integrity of SFEG layers at the optimal spray conditions. As the polymer dosages and membrane fluxed are both highly related to the film thickness, thinner BCP layers could lower the cost and improve fluxes. After completely dried in an oven at 100 °C for 30 min, the SFEG layers tightly attached on the nylon supports were intact and semitransparent (Fig. 2(e)), indicating the good strength and nonporous nature.

The adhesive force between the separation layers and supporting layers has been a vital concern to construct composite structures [34,35]. We note that the adhesion between SFEG layers and nylon supports was tight enough to withstand strong shake in water. In this study,

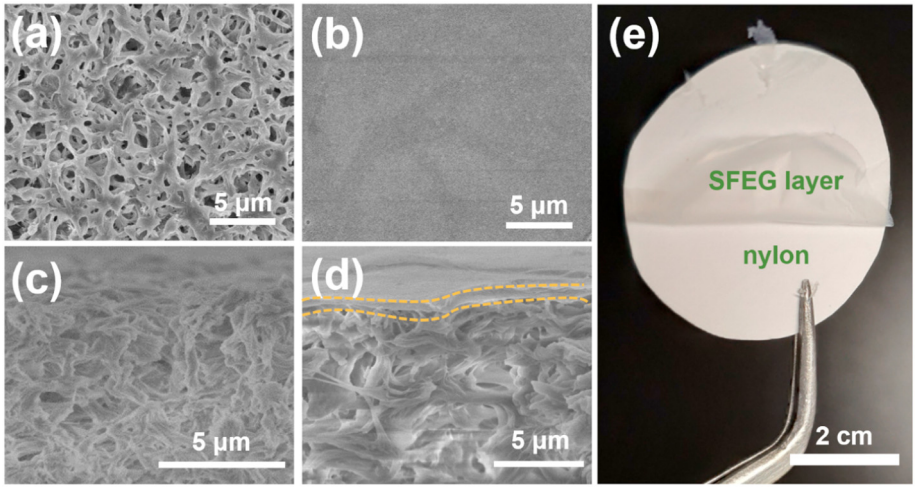

Fig. 2. Surface SEM images of (a) the nylon microfiltration supports and (b) the bi-layered composite films with SFEG atop nylon supports. (c) and (d) are the corresponding cross-sectional SEM images. (e) is the macroscopic image of the SFEG composite film. The triblock polymer coating layer was partially detached from the substrate to show the composite structure.

the adhesion between SFEG layers and nylon supports was roughly evaluated by treatment in ultrasonication in water at 100 W for 30 min. The SFEG-coated films remained their integrity and no detachment from supports was found. The composite membranes remained nonpermeable by tests in cross-flow apparatus at 0.1 MPa for 30 min after ultrasonication treatment, indicating that defect-free SFEG layers were tightly attached on nylon supports. The strong adhesion was considered to stem from the slight penetration of SFEG into nylon pores and the tight physical attachment of these SFEG with the nylon skeleton (Fig. 2(d)).

3.2. Pore generation by swelling in paired solvents

In order to effectively swell the SFEG polymers, paired solvents composed of ethanol and acetone were utilized as the swelling agent in this work. Due to the higher glass transition temperature and consequently weaker mobility of SFEG, the selective swelling induced pore generation of SFEG films was more difficult compared to PS-*b*-P2VP (abbreviated as S2VP) materials [36–38]. Mesoscale pores can be easily cavitated in S2VP thin films even if immerged in pure ethanol for a short duration. However, SFEG thin films remained dense while immerged in hot ethanol for a long duration. Acetone is a good solvent for PSF, it was chosen here to plasticize the PSF matrix and enhance the mobility of polymer chains during selective swelling process. In principle, the appropriate swelling agent should have good affinity for PEG so as to sufficiently swell the dispersed phases and have moderate affinity for PSF enabling the plastic deformation of the matrix phases. However, a single solvent cannot meet the demands for BCP of PSF-*b*-PEG. Therefore, solvent pair of ethanol and acetone was employed here, where the former is a good solvent for PEG and the latter is good solvent for PSF [21]. When soaked in the ethanol/acetone paired solvent, both PSF and PEG were swollen while the PEG chains were significantly expanded. Upon taken out from the solvent, the volume occupied by the expanded PEG was transformed into mesopores.

We studied the effects of different paired solvents on the structures and performances of the SFEG membranes. Different mass percentages of acetone, including 5%, 7%, 10%, 15%, 20%, 25%, and 30% content, were added into ethanol to obtain paired solvents. The nylon substrates spray coated with SFEG were subsequently immerged in the paired solvents for a certain duration to generate mesopores throughout the SFEG layers. The pore sizes as well as thicknesses of the SFEG layers were enlarged with the increase of acetone contents in paired solvents at 70 °C for 5 h, as shown in Fig. 3 and Fig. 4. The pore sizes of SFEG membranes were enlarged from 15.6 nm to 64.7 nm (Table S1). Few pores were distributed on the surface or cross section of the membranes when the acetone content was 5 wt% or 7 wt% (Fig. 3(a), (e) and Fig. S1). This is because the mobility of PSF chains in such paired solvents was poor and the mobilities of PEG chains were also confined. Selective swelling induced pore generation was not triggered. With the acetone content increased to 10 wt% and 15 wt%, the number of mesopores on the membrane surface was slightly increased and the cross-sectional views of membranes became porous (Fig. 3(b), (f) and Fig. S1) owing to the mobility enhancement of PSF chains at higher acetone percentages. Furthermore, mesopores spread throughout both the surface and cross section of the SFEG layers with the acetone mass content rising up to 20%, 25% and 30% (Fig. 3(c), (d), (g), (h) and Fig. S1). According to the mechanism of selective swelling, the swelling durations also have a significant effect on the pore generation [21,39]. As shown in Fig. S2, when the swelling durations were prolonged from 1 h to 3, 5 and 7 h with the acetone content maintained at 20 wt%, the pore sizes and porosities of the membranes were apparently enlarged with prolongation of swelling time at 70 °C. Moreover, micellization of SFEG began to take place when the swelling duration reached up to 7 h.

Fig. 4(a) gives the thickness of SFEG layers after swelling in different paired solvents. With the increase of acetone, the thickness of the SFEG layers was increased to 1.24, 1.26, 1.27, 1.37, 2.63, 2.74, and 2.91 μm, respectively. The porosity of SFEG layers was increased from 4.0% to 5.6%,6.3%,13.1%,54.8%,56.6% and 59.1% respectively with the acetone mass content increasing from 5% to 7%, 10%, 15%, 20%, 25%, and 30%, as shown in Fig. 4(b). Here the membrane thicknesses were related to the porosities, and these results agreed with our discussions above.

The membrane surface and pore walls became more hydrophilic and the water permeability was enhanced with the increased acetone contents from 5 wt% to 30 wt%. The presence of PEG chains decorating the PSF walls on porous surface improved the water permeability. As shown in Table S2, we detected the atomic and mass ratio of oxygen to sulfur by EDX, the increase of ratios of oxygen to sulfur demonstrated that the PEG domains migrated to the surface of SFEG membranes. Meanwhile, the initial water contact angle of non-swollen SEFG composite films was 84.5° and slowly stabilized at around 63.8° as shown in Fig. 4(c). For the membranes prepared by swelling in paired solvents composed of 5 wt% or 10 wt% acetone and swollen at 70 °C for 5 h, their water contact angles were almost unchanged, indicating that the SEFG polymer chains were mainly frozen under this condition. This was consistent with the inadequate cavitating ability of SFEG layers analyzed by SEM (as shown in Fig. 3(a), (b), (e) and (f)) when the content of acetone was below 10 wt%. With the content of acetone increasing to 20 wt% and 30 wt%, the water contact angles were decreased to 78.6° and 73°, respectively and the water drops quickly permeated into the SFEG composite membranes within ~17 and 12 s. The enhanced permeation and

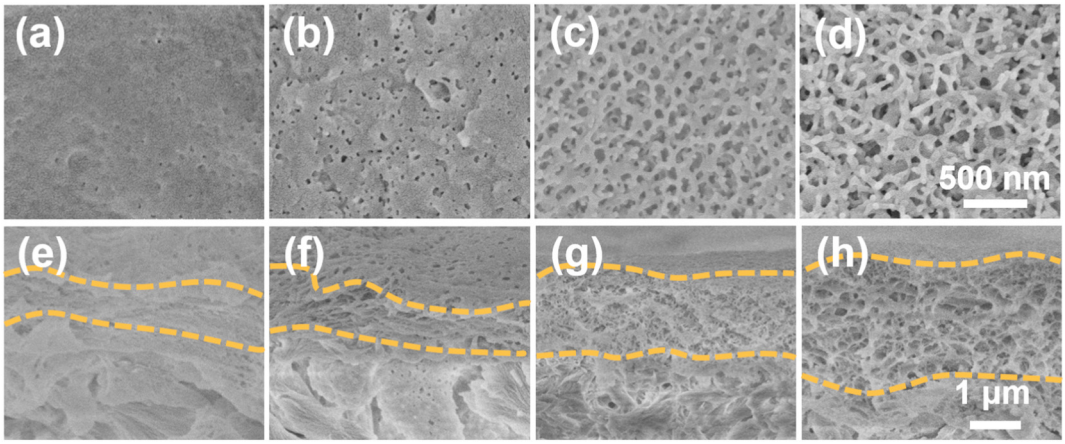

Fig. 3. SEM images of the SFEG composite membranes after swelling in ethanol/acetone paired solvents with different acetone content at 70 °C for 5 h: (a–d) top surface views, and (e–h) cross-sectional views for membranes prepared with 5 wt%, 10 wt%, 20 wt%, 30 wt% acetone content, respectively. Images of (a–d) have the same magnification and the scale bar corresponding to 500 mm is given in (d). Images of (e–h) have the same magnification and the scale bar corresponding to 1 μm is given in (h).

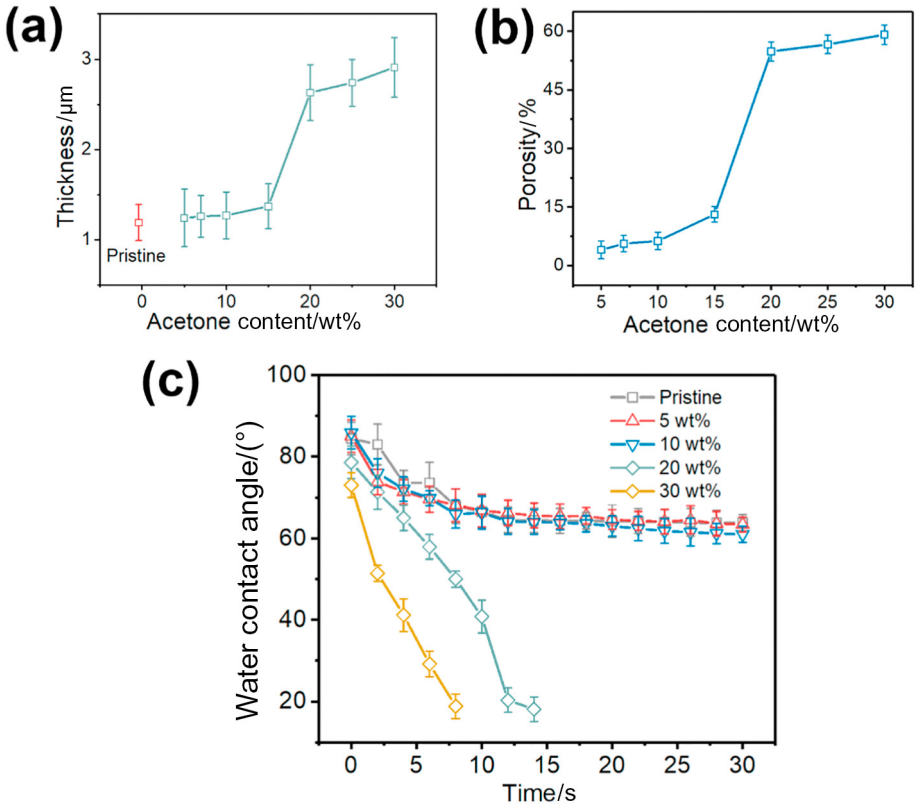

Fig. 4. (a) The thicknesses and (b) porosities of SFEG layers after swelling by different compositions of acetone at 70 °C for 5 h. (c) Dynamic water contact angles of the SFEG composite membranes subjected to different compositions of acetone swelling at 70 °C for 5 h.

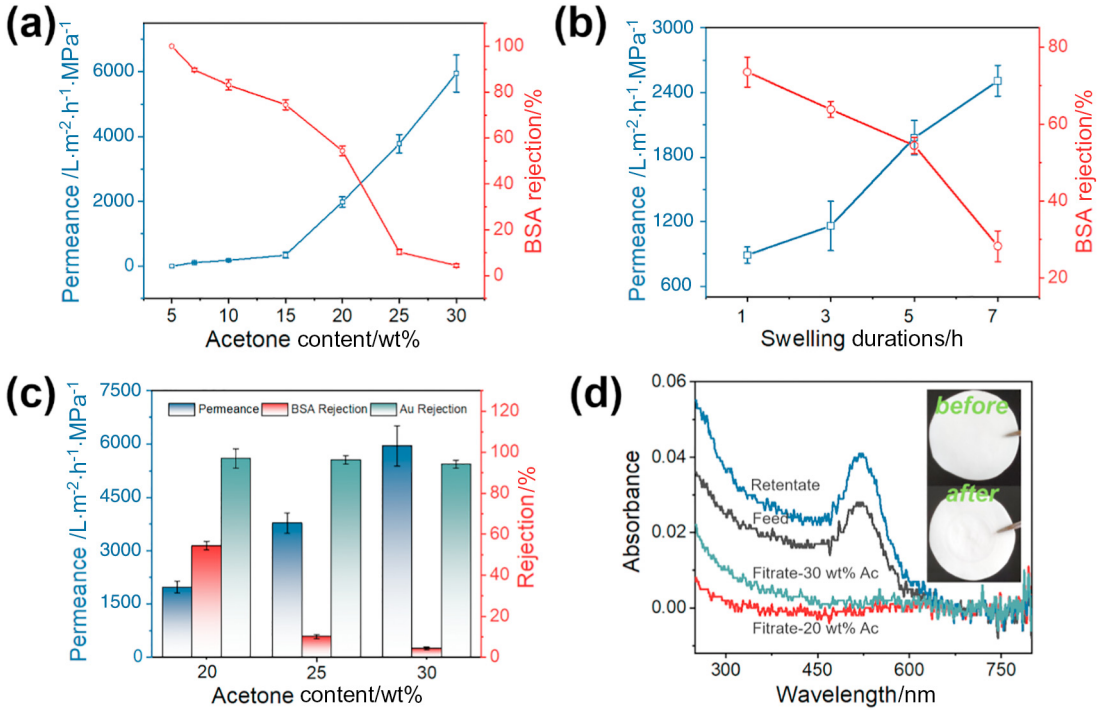

Fig. 5. The permeance and BSA rejection of the SFEG composite membranes: (a) after swelling in paired solvents with different acetone content at 70 °C for 5 h, (b) after swelling in paired solvent with 20 wt% acetone content at 70 °C for different durations. (c) The permeance and rejection (BSA and 15-nm gold nanoparticles) of the composite membranes after swelling in paired solvents with 20 wt%, 25 wt% and 30 wt% acetone content at 70 °C for 5 h. (d) UV–vis absorption spectra of the feed, filtrate, and retentate solutions of 15-nm gold nanoparticles through the SFEG composite membranes after swelling in 20 wt% and 30 wt%-acetone content solvents at 70 °C for 5 h. Insets in (d) are the photographs of the composite membranes before and after gold nanoparticle filtration tests.

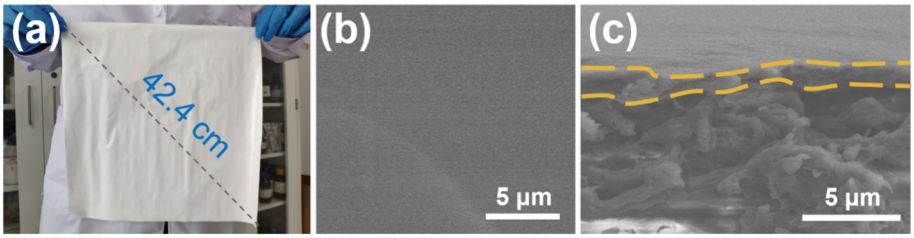

Fig. 6. The SFEG composite films prepared at large scale: (a) the digital photo, (b) the top surface SEM image, and (c) the cross-sectional SEM image.

hydrophilicity were ascribed to the pore formation as well as surface PEG enrichment at higher acetone contents.

3.3. UF performances of SFEG membranes

The separation performances of SFEG composite membranes were evaluated using BSA and gold nanoparticle solutions. The acetone contents in paired solvents play a vital role in generating mesopores throughout the SFEG layers and consequently result in different separation properties. As shown in Fig. 5(a), with the increase of acetone, the water permeance surged from 110 to 5950 $L \cdot m^{-2} \cdot h^{-1} \cdot MPa^{-1}$ and the BSA rejection rate sharply decreased from 89.6% to 4.4%, owing to the improved hydrophilicity and enlarged pores. The water permeance was relatively low when the acetone content was smaller than 15% while a great leap of water permeance can be observed with the acetone content coming up to 20%. These results are correlated well with the above discussion on pore generation, proving that acetone contents have a big effect on membrane performances. The performances were also tunable by swelling conditions. As shown in Fig. 5(b), the water permeance was increased from 890 to 2510 $L \cdot m^{-2} \cdot h^{-1} \cdot MPa^{-1}$, and the rejection to BSA reduced from 73.5% to 28.2% with the swelling durations prolonged from 1 to 7 h as stronger swelling led to larger pores. Here, the effect of swelling durations was performed with the acetone content fixed at 20 wt% and swelling temperature at 70 °C. With the promotion of water permeance, the BSA rejection rate decreased to 4.4%, but the composite membranes still remained a high rejection rate to gold nanoparticles with a diameter of 15 nm (Fig. 5(c)). We detected the gold nanoparticles concentrations in feed solutions, filtrates and retentates by UV–vis. As shown in Fig. 5(d), the absorbance intensity of gold nanoparticles in feeds was nearly zero while much higher in retentates, indicating that the SFEG composite membranes have an excellent size-exclusion ability and almost no adsorption to gold nanoparticles. Also, the surface of the SFEG composite membranes remained white and uncontaminated after gold nanoparticle filtration tests (Fig. 5(d)).

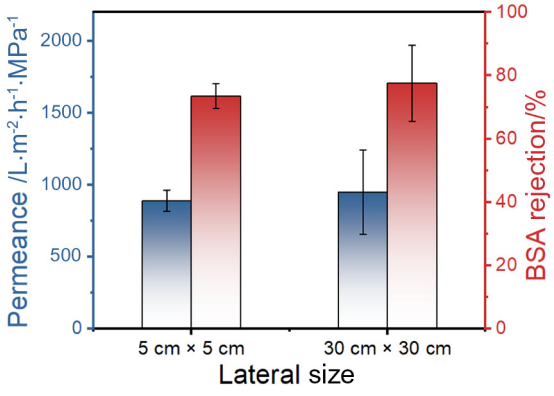

Fig. 7. The permeance and BSA rejection of the SFEG membranes in larger and smaller area after swelling in 20 wt% acetone paired solvent at 70 °C for 1 h.

The adhesion between the SFEG layers and nylon supports after swelling was also evaluated. The volume expanding of SFEG domains after swelling in dual-solvents, might weaken the adhesive force between the two layers of composite membranes. Herein, ultrasonication treatments were performed to assess the adhesion of the two layers. As shown in Fig. S3, no cracks or detachments of the SFEG layers from supports were observed from a macroscopic view. Besides, the ultrasonicated-composite membranes possessed almost identical water fluxes and BSA rejection rates compared with the non-ultrasonication membranes, indicating that the SFEG layers were firmly attached to nylon supports after swelling.

To explore the upscale ability of spray coating, larger microfiltration nylon substrates with a size of 30 cm × 30 cm were employed to fabricate SFEG composite films (Fig. 6(a)). Similar to Fig. 2(b) and (d), the macroporous structure of the nylon substrate was also completely covered by a thin, continuous and defect-free SFEG layer after spray coating (Fig. 6(b) and (c)). The thickness of SFEG layer was almost same with small-area fabrication about 1.15 μm. As shown in Fig. 7, the two composite membranes with smaller and larger size showed almost identical performances. This result demonstrated that larger SFEG membranes can be prepared at no expense of performances by spray coating and selective swelling. Moreover, as spray coating can be an uninterrupted process by moving the relative position of substrates, continuous preparation for composite membranes is possible by introducing a roll to roll process.

4. Conclusions

Here we propose a facile and up-scalable fabrication strategy for PSF/PEG triblock polymer membranes by spray coating enabled film formation and selective swelling induced pore generation. The composite membranes consist of macroporous supporting layers and thin SFEG separation layers, which can be as thin as 1.2 μm obtained at optimal spray conditions. The adhesion between the two layers is demonstrated to be tight. Because the PSF and PEG components are chemically bonded in this triblock polymer with PSF as the majority block, SFEG membranes show good mechanical strength, stability, and hydrophilicity. The pore sizes, porosities, hydrophilicity and UF performances of the membranes are tunable by altering the composition of paired swelling solvents and the swelling durations. Moreover, larger-area SFEG membranes can be easily prepared at no expense of separation performances, implying the upscalability of this “spraying coating + selective swelling” process.

Acknowledgements

Financial support from the National Natural Science Foundation of China (21706119) and the Program of Excellent Innovation Teams of Jiangsu Higher Education Institutions and the Project of Priority Academic Program Development of Jiangsu Higher Education Institutions (PAPD) is gratefully acknowledged. We also thank the partial support by the Open Fund of State Key Laboratory of Separation Membranes and Membrane Process (M1-201702).

Supplementary Material

Supplementary data to this article can be found online at https://doi.org/10.1016/j.cjche.2020.05.002.

References

[1] J.R. Werber, C.O. Osuji, M. Elimelech, Materials for next-generation desalination and water purification membranes, *Nat. Rev. Mater.* 1 (2016) 16018.
[2] J. Wu, F. Xu, S. Li, P. Ma, X. Zhang, Q. Liu, R. Fu, D. Wu, Porous polymers as multifunctional material platforms toward task-specific applications, *Adv. Mater.* 31 (2019), e1802922. .
[3] J.Y. Park, M.H. Acar, A. Akthakul, W. Kuhlman, A.M. Mayes, Polysulfone-graft-poly (ethylene glycol) graft copolymers for surface modification of polysulfone membranes, *Biomaterials* 27 (2006) 856–865.
[4] K. Zodrow, L. Brunet, S. Mahendra, D. Li, A. Zhang, Q. Li, P.J.J. Alvarez, Polysulfone ultrafiltration membranes impregnated with silver nanoparticles show improved biofouling resistance and virus removal, *Water Res.* 43 (2009) 715–723.
[5] V. Kochkodan, N. Hilal, A comprehensive review on surface modified polymer membranes for biofouling mitigation, *Desalination* 356 (2015) 187–207.
[6] Y.Q. Song, J. Sheng, M. Wei, X.B. Yuan, Surface modification of polysulfone membranes by low-temperature plasma–graft poly(ethylene glycol) onto polysulfone membranes, *J. Appl. Polym. Sci.* 78 (2000) 979–985.
[7] Y. Yang, H. Zhang, P. Wang, Q. Zheng, J. Li, The influence of nano-sized TiO2 fillers on the morphologies and properties of PSF UF membrane, *J. Membr. Sci.* 288 (2007) 231–238.
[8] Q.Z. Zheng, P. Wang, Y.-N. Yang, Rheological and thermodynamic variation in polysulfone solution by PEG introduction and its effect on kinetics of membrane formation via phase-inversion process, *J. Membr. Sci.* 279 (2006) 230–237.
[9] J.H. Kim, K.H. Lee, Effect of PEG additive on membrane formation by phase inversion, *J. Membr. Sci* 138 (1998) 153–163.
[10] S. Hou, X. Wang, X. Dong, J. Zheng, S. Li, Renewable antibacterial and antifouling polysulfone membranes incorporating a PEO-grafted amphiphilic polymer and N-chloramine functional groups, *J. Colloid Interface Sci.* 554 (2019) 658–667.
[11] S. Zhao, Z. Wang, X. Wei, B. Zhao, J. Wang, S. Yang, S. Wang, Performance improvement of polysulfone ultrafiltration membrane using well-dispersed polyaniline–poly(vinylpyrrolidone) nanocomposite as the additive, *Ind. Eng. Chem. Res.* 51 (2012) 4661–4672.
[12] M.J. Han, Effect of propionic acid in the casting solution on the characteristics of phase inversion polysulfone membranes, *Desalination* 121 (1999) 31–39.
[13] G.R. Guillen, T.P. Farrell, R.B. Kaner, E.M.V. Hoek, Pore-structure, hydrophilicity, and particle filtration characteristics of polyaniline–polysulfone ultrafiltration membranes, *J. Mater. Chem.* 20 (2010) 4621–4628.
[14] Z. Fan, Z. Wang, N. Sun, J. Wang, S. Wang, Performance improvement of polysulfone ultrafiltration membrane by blending with polyaniline nanofibers, *J. Membr. Sci.* 320 (2008) 363–371.
[15] J.H. Kim, K.H. Lee, Effect of PEG additive on membrane formation by phase inversion, *J. Membr. Sci.* 138 (1998) 153–163.
[16] I.C. Kim, K.H. Lee, Effect of poly(ethylene glycol) 200 on the formation of a polyetherimide asymmetric membrane and its performance in aqueous solvent mixture permeation, *J. Membr. Sci.* 230 (2004) 183–188.
[17] Y. Chen, M. Wei, Y. Wang, Upgrading polysulfone ultrafiltration membranes by blending with amphiphilic block copolymers: Beyond surface segregation, *J. Membr. Sci.* 505 (2016) 53–60.
[18] C. Shen, Q. Meng, G. Zhang, Chemical modification of polysulfone membrane by polyethylene glycol for resisting drug adsorption and self-assembly of hepatocytes, *J. Membr. Sci.* 369 (2011) 474–481.
[19] W. Chen, M. Wei, Y. Wang, Advanced ultrafiltration membranes by leveraging microphase separation in macrophase separation of amphiphilic polysulfone block copolymers, *J. Membr. Sci.* 525 (2017) 342–348.
[20] D. Zhong, Z. Wang, Q. Lan, Y. Wang, Selective swelling of block copolymer ultrafiltration membranes for enhanced water permeability and fouling resistance, *J. Membr. Sci.* 558 (2018) 106–112.
[21] Z. Wang, R. Liu, H. Yang, Y. Wang, Nanoporous polysulfones with in situ PEGylated surfaces by a simple swelling strategy using paired solvents, *Chem. Commun.* 53 (2017) 9105–9108.
[22] H. Yang, J. Zhou, Z. Wang, X. Shi, Y. Wang, Selective swelling of polysulfone/poly (ethylene glycol) block copolymer towards fouling-resistant ultrafiltration membranes, *Chin. J. Chem. Eng.* 28 (2020) 98–103.
[23] T. Bucher, V. Filiz, C. Abetz, V. Abetz, Formation of Thin, isoporous block copolymer membranes by an upscalable profile roller coating process—A promising way to save block copolymer, *Membranes* 8 (2018) 57–73.
[24] S.Y. Yang, I. Ryu, H.Y. Kim, J.K. Kim, S.K. Jang, T.P. Russell, Nanoporous membranes with ultrahigh selectivity and flux for the filtration of viruses, *Adv. Mater.* 18 (2006) 709–712.
[25] D. Ma, J. Zhou, Z. Wang, Y. Wang, Block copolymer ultrafiltration membranes by spray coating coupled with selective swelling, *J. Membr. Sci.* 598 (2020) 117656.
[26] A.T. Barrows, A.J. Pearson, C.K. Kwak, A.D.F. Dunbar, A.R. Buckley, D.G. Lidzey, Efficient planar heterojunction mixed-halide perovskite solar cells deposited via spray-deposition, *Energy Environ. Sci.* 7 (2014) 2944–2950.
[27] F. Aziz, A.F. Ismail, Spray coating methods for polymer solar cells fabrication: A review, *Mater. Sci. Semicond. Process.* 39 (2015) 416–425.
[28] A. Reale, L.L. Notte, L. Salamandra, G. Polino, G. Susanna, T.M. Brown, F. Brunetti, A.D. Carlo, Spray coating for polymer solar cells: an up-to-date overview, *Energy Technol.* 3 (2015) 385–406.
[29] D. Vak, S. Kim, J. Jo, S. Oh, S. Na, J. Kim, D. Kim, Fabrication of organic bulk heterojunction solar cells by a spray deposition method for low-cost power generation, *Appl. Phys. Lett.* 91 (2007), 081102. .
[30] Z. Tan, S. Chen, X. Peng, L. Zhang, C. Gao, Polyamide membranes withnanoscale turing structures forwater purification, *Science* 360 (2018) 518–521.
[31] Z. Wang, Z. Wang, S. Lin, H. Jin, S. Gao, Y. Zhu, J. Jin, Nanoparticle-templated nanofiltration membranes for ultrahigh performance desalination, *Nat. Commun.* 9 (2018) 2004.
[32] N. Wang, T. Wang, Y. Hu, Tailoring membrane surface properties and ultrafiltration performances via the self-assembly of polyethylene glycol-block-polysulfone-block-polyethylene glycol block copolymer upon thermal and solvent annealing, *ACS Appl. Mater. Interfaces* 9 (2017) 31018–31030.
[33] L. Saitoh, R.R. Babu, S. Kannappan, K. Kojima, T. Mizutani, S. Ochiai, Performance of spray deposited poly [N-9″-hepta-decanyl-2,7-carbazole-alt-5,5-(4′,7′-di-2-thienyl-2′,1′,3′-benzothiadiazole)]/[6,6]-phenyl-C61-butyric acid methyl ester blend active layer based bulk heterojunction organic solar cell devices, *Thin Solid Films* 520 (2012) 3111–3117.
[34] X. Yao, Z. Wang, Z. Yang, Y. Wang, Energy-saving, responsive membranes with sharp selectivity assembled from micellar nanofibers of amphiphilic block copolymers, *J. Mater. Chem. A* 1 (2013) 7100.
[35] X. Yao, J. Li, Z. Wang, L. Kong, Y. Wang, Highly permeable and robust membranes assembled from block-copolymer-functionalized carbon nanotubes, *J. Membr. Sci.* 493 (2015) 224–231.
[36] Z. Wang, X. Yao, Y. Wang, Swelling-induced mesoporous block copolymer membranes with intrinsically active surfaces for size-selective separation, *J. Mater. Chem.* 22 (2012) 20542.
[37] J. Yin, X. Yao, J.Y. Liou, W. Sun, Y.S. Sun, Y. Wang, Membranes with highly ordered straight nanopores by selective swelling of fast perpendicularly aligned block copolymers, *ACS Nano* 7 (2013) 9961–9974.
[38] N. Yan, Y. Wang, Selective swelling induced pore generation of amphiphilic block copolymers: The role of swelling agents, *J. Polym. Sci. B Polym. Phys.* 54 (2016) 926–933.
[39] Y. Wang, Nondestructive creation of ordered nanopores by selective swelling of block copolymers: Toward homoporous membranes, *Acc. Chem. Res.* 49 (2016) 1401–1408.